

# ESP-ELS and ESP-HS modules

Focused processing of hot (OBA)  
& emission-line stars for Gaia DR3

Y. Frémat<sup>1</sup>

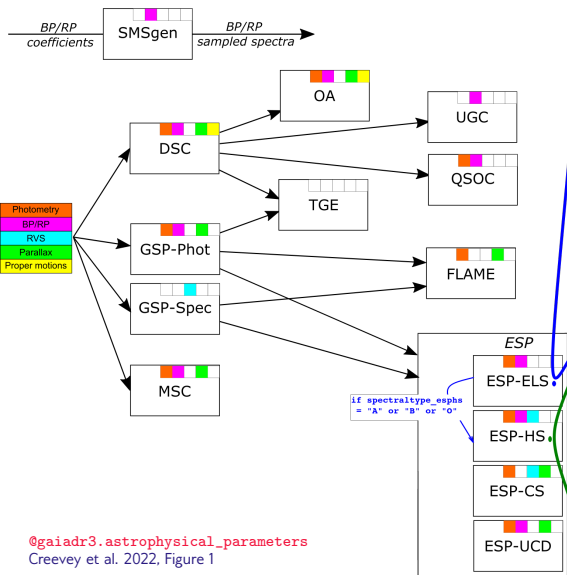
<sup>1</sup>Royal observatory of Belgium (ROB)

With direct contributions from:

A. Lobel (ROB), C. Martayan (ESO),  
J. Zorec (IAP), A. Jonckheere



# Apsis & ESP Workflows

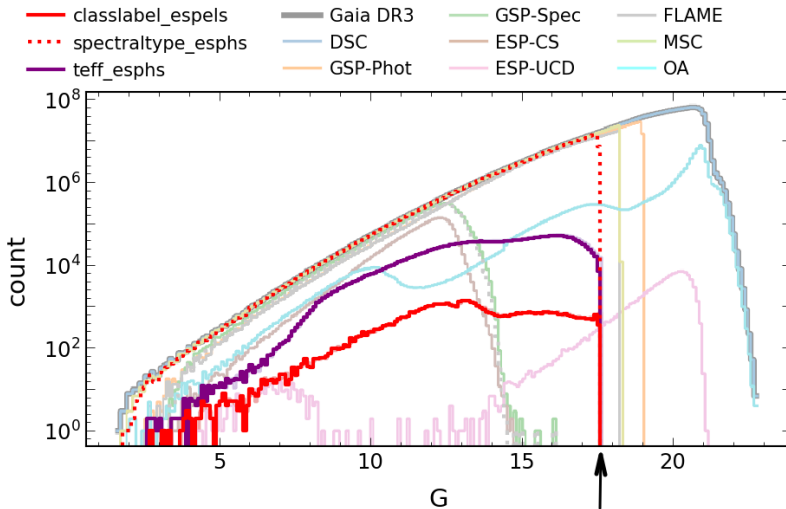


- Extended Stellar Parametrizer: ELS (Emission-Line Stars) and HS (Hot Stars)

- spectraltypes\_espels
- classlabel\_espels, classprob\_espels...
- ew\_espels\_halpaha, ew\_espels\_halpaha\_model, ew\_espels\_halpaha\_flag
- teff\_espels, logg\_espels, azero\_espels, ag\_espels, ebpminrp\_espels, (vsini\_espels)

@gaiadr3.astrophysical\_parameters  
Creevey et al. 2022, Figure 1

# Output: Magnitude Distribution



Adapted from Creevey et al. 2022, Figure 2

ESP-ELS/HS magnitude cut at G=17.65

# Presentation Outline

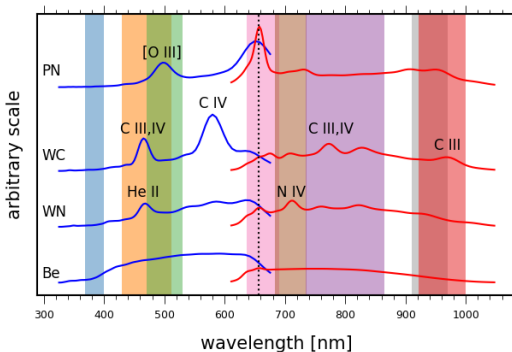
- ESP-ELS
  - Methods
  - Results
- ESP-HS
  - Methods
  - Results
- Overview & DR3 to DR4



# Classification of Emission-Line Stars (ELS): Methodology

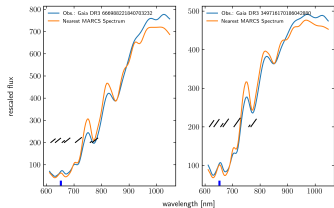
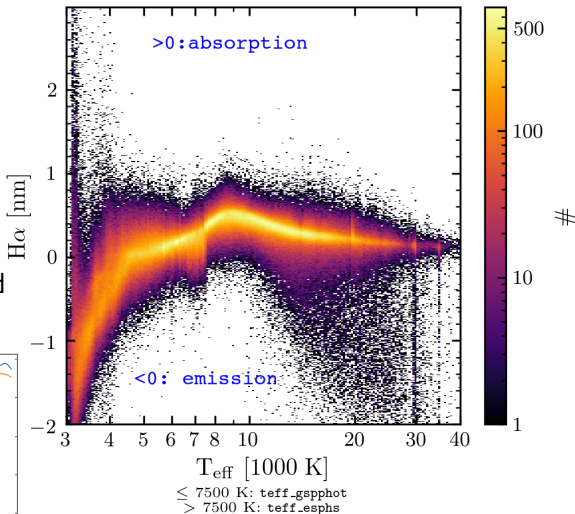
- Apsis only processes co-added spectra, not externally calibrated
- Division by a mean 'response' curve
- Extraction main emission features in the BP and RP
- Locally normalize these
- Combine with GSP-Phot APs (before post-processing) for ELS classlabel

Creevey et al. 2022, Figure 8



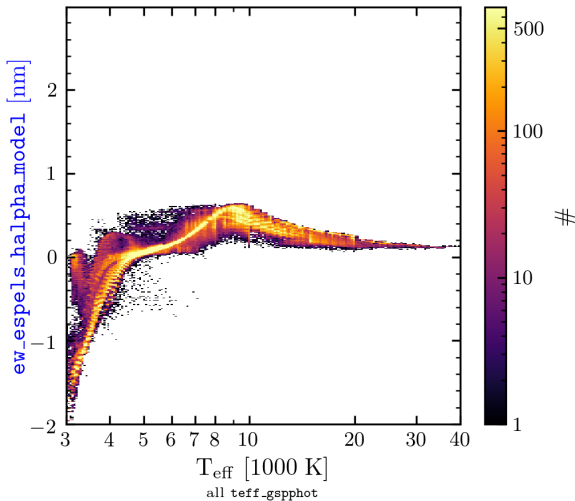
# Measurement of $H\alpha$ pseudo-Equivalent Width (pEW)

- Facts: at (RP)  $H\alpha$  resolution 8 nm and 2.5 nm samples
- Measurement band: 646 - 670 nm.
- No  $H\alpha$  absorption in M and K stars, but molecule blends bend the continuum.



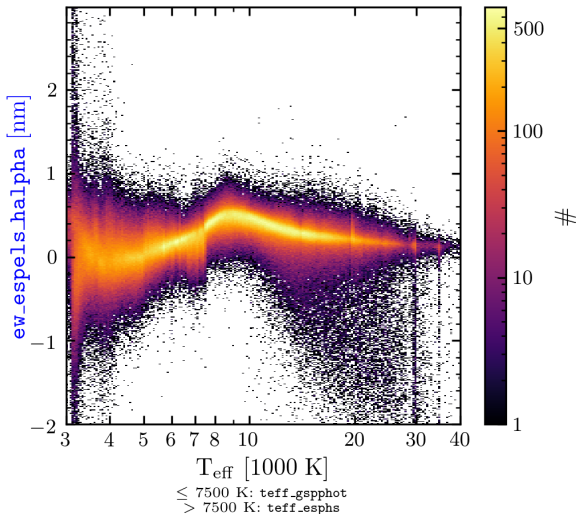
# H $\alpha$ pEW (model $\infty$ GSP-Phot APs)

- $\sim 2$  M. random targets uniformly distributed over  $T_{\text{eff}}$
- Variations seen in synthetic spectra.
- GSP-Phot APs available (i.e. before post-processing) when H $\alpha$  is measured
- Model value used to 'correct' at  $T_{\text{eff}} \leq 5000\text{K}$ .



# H $\alpha$ pEW ('corrected' $\infty$ GSP-Phot APs)

- `ew_espels`  
`_halpha_flag`: 0  
 (model not subtracted), 1  
 (model subtracted)
- stored in  
`ew_espels`  
`_halpha`
- `ew_espels`  
`_halpha_model`  
 allways present
- pEW used to  
 trigger/identify ELS

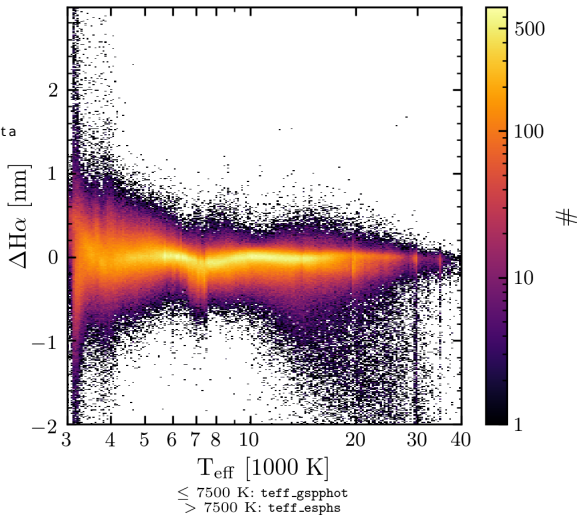


# H $\alpha$ pEW (all 'corrected' $\infty$ GSP-Phot APs)

```

SELECT
TOP 50
source_id ,
teff_gspphot ,
teff_esphs ,
(ew_espels_halpha
-ew_espels_halpha_model) AS delta
FROM
gaiadr3.astrophysical_parameters
WHERE
ew_espels_halpha IS NOT NULL AND
ew_espels_halpha_flag = '0'
UNION
SELECT
TOP 50
source_id ,
teff_gspphot ,
teff_esphs ,
ew_espels_halpha AS delta
FROM
gaiadr3.astrophysical_parameters
WHERE
ew_espels_halpha IS NOT NULL AND
ew_espels_halpha_flag = '1'

```

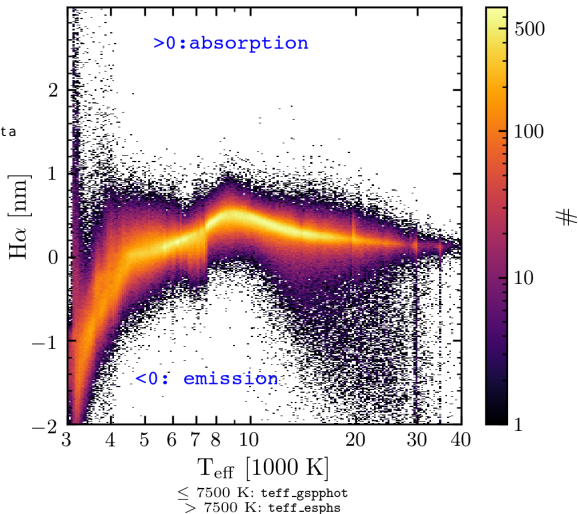


# H $\alpha$ pEW (return to measurement)

```

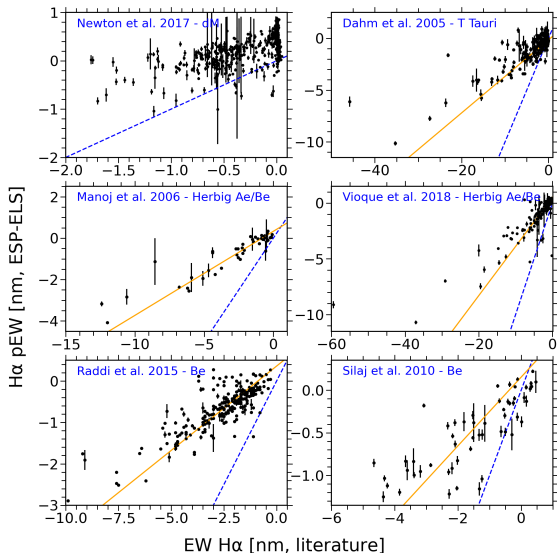
SELECT
TOP 50
source_id ,
teff_gspphot ,
teff_esphs ,
(ew_espels_halpha
+ew_espels_halpha_model) AS delta
FROM
gaiadr3.astrophysical_parameters
WHERE
ew_espels_halpha IS NOT NULL AND
ew_espels_halpha_flag = '1'
UNION
SELECT
TOP 50
source_id ,
teff_gspphot ,
teff_esphs ,
ew_espels_halpha AS delta
FROM
gaiadr3.astrophysical_parameters
WHERE
ew_espels_halpha IS NOT NULL AND
ew_espels_halpha_flag = '0'

```



Gaia DR3  $H\alpha$  pseudo-Equivalent Width vs  $H\alpha$ 

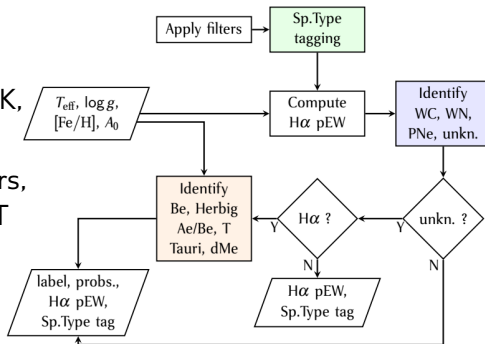
- blue: 1-1 relation
- value 2 to 3 times smaller than expected, worse for M and K stars.
- comparisons with LAMOST: see Shridharan et al. 2022, AA, 668, A156



Fouesneau et al. 2022, Figure 21

# ESP-ELS: Labelling Workflow

- Three RF classifiers all trained on synthetic and observed data.
- Spectral type tag (`spectraltype_esphs`): M, K, .... B, O, CSTAR
- Identification of WC/WN stars, PN, then Be, Herbig Ae/Be, T Tauri, and active M dwarf stars.
- `classlabel_espels` and `classlabel_espels_flag`
- `classprob_*`

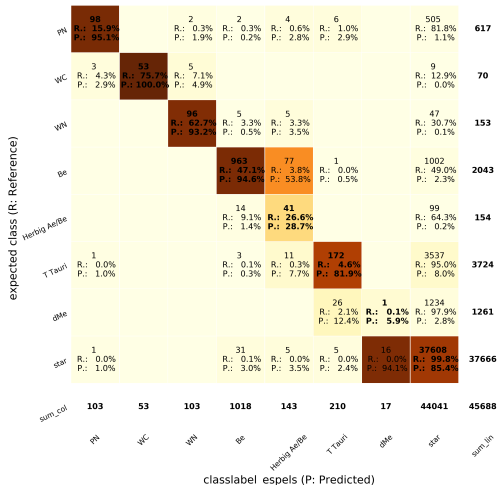


Online Doc. Sect. 11.3.7, Figure 11.37



# ESP-ELS: classlabel Confusion Matrix

- R/P: horizontally/vertically sums up. Color shades vary with P.
- Most PNs, TTauris and dMes lost, half of Be and Ae/Be stars identified
- Classifier most reliable for Be, WC.
- No filtering during the post-processing.
- `classlabel_espls_flag`: 1 - 4 (50 % probability if  $\leq 2$ ).
  - +10 if APs not consistent with `spectraltype_espls`
  - +20 if APs removed from Gaia DR3 after post-processing.



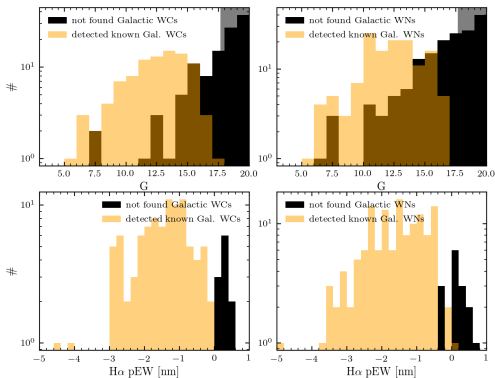
## ESP-ELS: classlabel

Fouesneau et al. 2022

**Table 2.** Number of identified candidates per ELS class and per quality flag (QF) value. QF  $\leq 2$  implies a probability larger than 50%.

| Class   | classlabel_espels_flag (QF) |      |      |      |      |       |       |
|---------|-----------------------------|------|------|------|------|-------|-------|
|         | 0                           | 1    | 2    | 3    | 4    | 10-14 | 20-24 |
| Be      | 3210                        | 3118 | 2815 | 2332 | 1475 | 122   | 3879  |
| Ae/Be   | 35                          | 94   | 231  | 519  | 972  | 299   | 1754  |
| T Tauri | 914                         | 2052 | 1594 | 1083 | 740  | 1180  | 27594 |
| dMe     | 0                           | 1    | 5    | 54   | 178  | 43    | 380   |
| PN      | 37                          | 52   | 83   | 85   | 16   | 0     | 0     |
| WC      | 106                         | 13   | 8    | 7    | 2    | 0     | 0     |
| WN      | 173                         | 38   | 29   | 142  | 47   | 0     | 0     |

- 57939 not null  
classlabel\_espels
- classlabel\_espels  
\_flag  $\leq 2$
- See Online Doc. Sect. 11.3.7  
(Results), e.g. Figure 11.41



# spectraltype\_esphs vs Simbad

Simbad (true, G < 18, qf ≤ 1)

|   | O                           | B                             | A                             | F                             | G                             | K                            | M                             | C                            |
|---|-----------------------------|-------------------------------|-------------------------------|-------------------------------|-------------------------------|------------------------------|-------------------------------|------------------------------|
| O | 316<br>R.: 47.6<br>P.: 52.6 | 330<br>(49.7)<br>(0.6)        | 5<br>(0.8)<br>(0.0)           | 10<br>(1.5)<br>(0.0)          | 1<br>(0.2)<br>(0.0)           | 1<br>(0.2)<br>(0.0)          | 1<br>(0.2)<br>(0.0)           |                              |
| B | 267<br>(0.6)<br>(44.4)      | 41646<br>R.: 90.3<br>P.: 70.0 | 3718<br>(8.1)<br>(5.3)        | 428<br>(0.9)<br>(0.4)         | 23<br>(0.0)<br>(0.1)          | 5<br>(0.0)<br>(0.1)          | 14<br>(0.0)<br>(0.0)          |                              |
| A | 2<br>(0.0)<br>(0.3)         | 16449<br>(19.9)<br>(27.6)     | 61978<br>R.: 74.9<br>P.: 89.1 | 4272<br>(5.2)<br>(4.2)        | 54<br>(0.1)<br>(0.3)          | 11<br>(0.0)<br>(0.1)         | 19<br>(0.0)<br>(0.1)          |                              |
| F | 3<br>(0.0)<br>(0.5)         | 857<br>(1.0)<br>(1.4)         | 3580<br>(4.1)<br>(5.1)        | 82487<br>R.: 93.4<br>P.: 80.5 | 1377<br>(1.6)<br>(7.3)        | 24<br>(0.0)<br>(0.3)         | 12<br>(0.0)<br>(0.0)          | 1<br>(0.0)<br>(0.0)          |
| G | 8<br>(0.0)<br>(1.3)         | 149<br>(0.5)<br>(0.3)         | 182<br>(0.6)<br>(0.3)         | 13963<br>(45.7)<br>(13.5)     | 15973<br>R.: 52.3<br>P.: 84.3 | 196<br>(0.6)<br>(2.1)        | 50<br>(0.2)<br>(0.1)          |                              |
| K | 1<br>(0.0)<br>(0.2)         | 69<br>(0.6)<br>(0.1)          | 103<br>(0.9)<br>(0.1)         | 926<br>(8.3)<br>(0.9)         | 1504<br>(13.5)<br>(7.9)       | 8007<br>R.: 71.9<br>P.: 85.3 | 530<br>(4.8)<br>(1.5)         | 4<br>(0.0)<br>(0.0)          |
| M | 4<br>(0.0)<br>(0.7)         | 11<br>(0.0)<br>(0.0)          | 14<br>(0.0)<br>(0.0)          | 51<br>(0.1)<br>(0.0)          | 20<br>(0.1)<br>(0.1)          | 750<br>(8.0)<br>(8.0)        | 33795<br>R.: 97.5<br>P.: 97.5 | 27<br>(0.1)<br>(0.3)         |
| C |                             |                               | 1<br>(0.0)<br>(0.0)           | 1<br>(0.0)<br>(0.0)           |                               | 394<br>(4.2)<br>(0.3)        | 95<br>(1.0)<br>(0.3)          | 9302<br>R.: 95.0<br>P.: 99.7 |

spectraltype\_esphs (predicted)

Simbad (true, G < 18, qf ≤ 5)

|   | O                            | B                             | A                             | F                              | G                             | K                              | M                             | C                            |
|---|------------------------------|-------------------------------|-------------------------------|--------------------------------|-------------------------------|--------------------------------|-------------------------------|------------------------------|
| O | 1070<br>R.: 49.5<br>P.: 35.1 | 933<br>(43.1)<br>(1.3)        | 11<br>(0.5)<br>(0.0)          | 22<br>(1.0)<br>(0.0)           | 3<br>(0.1)<br>(0.0)           | 32<br>(1.5)<br>(0.0)           | 85<br>(3.9)<br>(0.1)          | 7<br>(0.3)<br>(0.1)          |
| B | 1539<br>(2.8)<br>(50.5)      | 47013<br>R.: 84.3<br>P.: 64.4 | 5381<br>(9.6)<br>(5.9)        | 990<br>(1.8)<br>(0.7)          | 429<br>(0.8)<br>(0.7)         | 311<br>(0.6)<br>(0.2)          | 98<br>(0.2)<br>(0.2)          | 7<br>(0.0)<br>(0.1)          |
| A | 38<br>(0.0)<br>(1.2)         | 22736<br>(20.5)<br>(31.1)     | 77619<br>R.: 70.1<br>P.: 84.4 | 9285<br>(8.4)<br>(6.8)         | 283<br>(0.3)<br>(0.5)         | 669<br>(0.6)<br>(0.4)          | 75<br>(0.1)<br>(0.1)          |                              |
| F | 49<br>(0.0)<br>(1.6)         | 1750<br>(1.4)<br>(2.4)        | 8358<br>(6.9)<br>(9.1)        | 101675<br>R.: 83.9<br>P.: 73.9 | 7713<br>(6.4)<br>(13.1)       | 1585<br>(1.3)<br>(0.8)         | 75<br>(0.1)<br>(0.1)          | 4<br>(0.0)<br>(0.0)          |
| G | 52<br>(0.0)<br>(1.7)         | 363<br>(0.3)<br>(0.5)         | 392<br>(0.3)<br>(0.4)         | 23637<br>(20.9)<br>(17.2)      | 44859<br>R.: 39.7<br>P.: 76.0 | 43337<br>(38.4)<br>(22.9)      | 208<br>(0.2)<br>(0.3)         | 6<br>(0.0)<br>(0.1)          |
| K | 87<br>(0.1)<br>(2.9)         | 135<br>(0.1)<br>(0.2)         | 187<br>(0.1)<br>(0.2)         | 1775<br>(1.3)<br>(1.3)         | 5481<br>(3.9)<br>(9.3)        | 127120<br>R.: 90.9<br>P.: 67.1 | 5019<br>(3.6)<br>(7.8)        | 38<br>(0.0)<br>(0.4)         |
| M | 188<br>(0.3)<br>(6.2)        | 73<br>(0.1)<br>(0.1)          | 30<br>(0.0)<br>(0.0)          | 107<br>(0.2)<br>(0.1)          | 254<br>(0.4)<br>(0.4)         | 10408<br>(15.0)<br>(5.5)       | 58008<br>R.: 83.8<br>P.: 89.8 | 174<br>(0.3)<br>(1.8)        |
| C | 22<br>(0.1)<br>(0.7)         | 2<br>(0.0)<br>(0.0)           | 2<br>(0.0)<br>(0.0)           | 13<br>(0.1)<br>(0.0)           | 21<br>(0.1)<br>(0.0)          | 5986<br>(36.6)<br>(3.2)        | 970<br>(5.9)<br>(1.5)         | 9839<br>R.: 57.1<br>P.: 97.3 |

spectraltype\_esphs (predicted)

- `qf=flags_esphs[1:2]`
- color shades vary vertically, with lower (P) percentage in the cell
- contamination from neighbour types expected, but much stronger between O and B types

## spectraltype\_esphs vs LAMOST DR6

Xiang et al. 2022

Xiang et al. 2022 (true,  $G < 18$ ,  $qf \leq 1$ )

|   |                                    |                                      |                                      |                                     |                       |                       |                      |
|---|------------------------------------|--------------------------------------|--------------------------------------|-------------------------------------|-----------------------|-----------------------|----------------------|
| O | <b>158</b><br>R.: 29.8<br>P.: 68.1 | 234<br>(44.1)<br>(0.9)               | 118<br>(22.2)<br>(0.1)               | 21<br>(4.0)<br>(0.5)                |                       |                       |                      |
| B | 66<br>(0.2)<br>(28.4)              | <b>23044</b><br>R.: 80.6<br>P.: 83.8 | 5189<br>(18.2)<br>(4.9)              | 246<br>(0.9)<br>(6.1)               | 18<br>(0.1)<br>(38.3) | 12<br>(0.0)<br>(29.3) | 9<br>(0.0)<br>(56.2) |
| A | 8<br>(0.0)<br>(3.4)                | 3835<br>(3.7)<br>(13.9)              | <b>98052</b><br>R.: 95.6<br>P.: 91.7 | 565<br>(0.6)<br>(14.0)              | 22<br>(0.0)<br>(46.8) | 25<br>(0.0)<br>(61.0) | 6<br>(0.0)<br>(37.5) |
| F |                                    | 383<br>(5.4)<br>(1.4)                | 3532<br>(49.5)<br>(3.3)              | <b>3212</b><br>R.: 45.0<br>P.: 79.4 | 7<br>(0.1)<br>(14.9)  | 4<br>(0.1)<br>(9.8)   | 1<br>(0.0)<br>(6.2)  |
| G |                                    |                                      |                                      |                                     |                       |                       |                      |
| K |                                    |                                      |                                      |                                     |                       |                       |                      |
| M |                                    |                                      |                                      |                                     |                       |                       |                      |
|   | O                                  | B                                    | A                                    | F                                   | G                     | K                     | M                    |

spectraltype\_esphs (predicted)

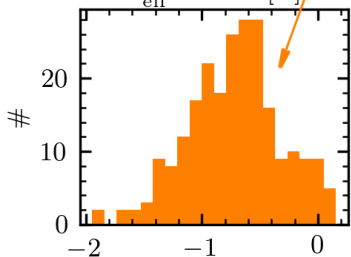
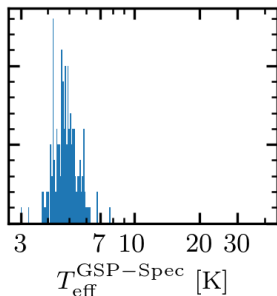
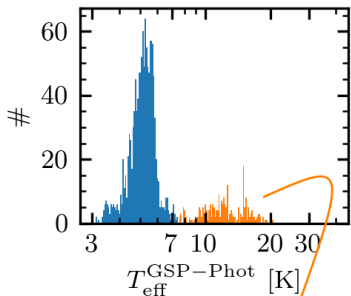
Xiang et al. 2022 (true,  $G < 18$ ,  $qf \leq 9$ )

|   |                                    |                                      |                                       |                                      |                        |                        |                       |
|---|------------------------------------|--------------------------------------|---------------------------------------|--------------------------------------|------------------------|------------------------|-----------------------|
| O | <b>662</b><br>R.: 36.8<br>P.: 52.7 | 666<br>(37.0)<br>(1.0)               | 291<br>(16.2)<br>(0.1)                | 83<br>(4.6)<br>(0.3)                 | 76<br>(4.2)<br>(9.5)   | 21<br>(1.2)<br>(2.2)   | 2<br>(0.1)<br>(1.7)   |
| B | 473<br>(0.7)<br>(37.7)             | <b>43677</b><br>R.: 67.3<br>P.: 66.9 | 17297<br>(26.7)<br>(7.9)              | 2657<br>(4.1)<br>(8.1)               | 362<br>(0.6)<br>(45.4) | 362<br>(0.6)<br>(38.0) | 34<br>(0.1)<br>(29.6) |
| A | 104<br>(0.1)<br>(8.3)              | 19430<br>(9.6)<br>(29.8)             | <b>172777</b><br>R.: 85.1<br>P.: 78.7 | 9801<br>(4.8)<br>(29.9)              | 269<br>(0.1)<br>(33.7) | 489<br>(0.2)<br>(51.4) | 69<br>(0.0)<br>(60.0) |
| F | 17<br>(0.0)<br>(1.4)               | 1466<br>(2.9)<br>(2.2)               | 29037<br>(57.0)<br>(13.2)             | <b>20274</b><br>R.: 39.8<br>P.: 61.8 | 91<br>(0.2)<br>(11.4)  | 80<br>(0.2)<br>(8.4)   | 10<br>(0.0)<br>(8.7)  |
| G |                                    |                                      |                                       |                                      |                        |                        |                       |
| K |                                    |                                      |                                       |                                      |                        |                        |                       |
| M |                                    |                                      |                                       |                                      |                        |                        |                       |
|   | O                                  | B                                    | A                                     | F                                    | G                      | K                      | M                     |

spectraltype\_esphs (predicted)

- Xiang et al's  $T_{\text{eff}}$  converted into spectral type tag. See Table A.1 in Creevey et al. 2022.
- 320 578 with ESP tag. 1865 received a G,K or M tag ...

## spectraltype\_esphs vs LAMOST DR6

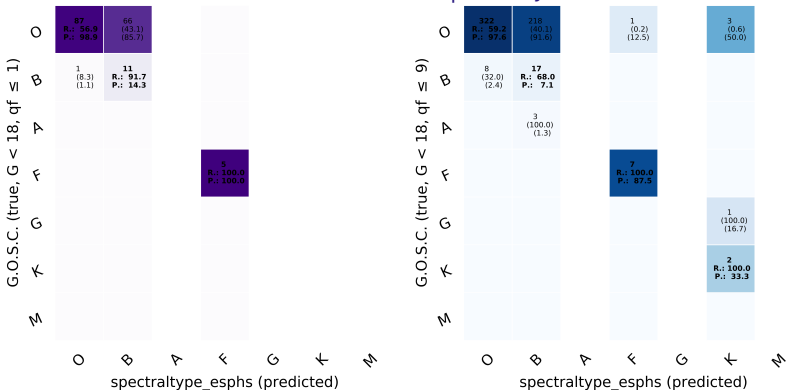


- 320 578 with ESP tag. 1865 received a G,K or M tag ...
- Tag more consistent with GDR3 results
- Wrong tag: probably due to x-match issues or due to emission.

$\text{ew\_espels\_halpha}$   
 $-\text{ew\_espels\_halpha\_model}$

# spectraltypes\_esphs vs Galactic O Star Catalogue

GOSC: Maíz Apellániz, J. et al. (2013)



- input list of 620 targets (main & supps). 582 found (21 too faint, 7 XP poor quality, 9 ?)
- filtering on `qf=flags_esphs[1:2]`: no significant impact on classification quality.
- strong O/B contamination (not depending on  $R_V$  nor  $A_V$ )

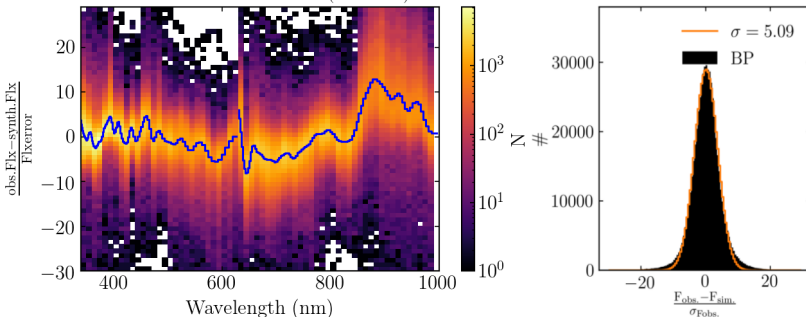
# AP Determination with ESP-HS

- Synthetic spectrum fit to XP and RVS data (when available).
- rebinned to 3 samples
- Libs.: O. Kochukhov & D. Shulyak, OB star models (Lanz & Hubeny), Synspec
- Assumption: Solar chemical composition

# AP Determination with ESP-HS

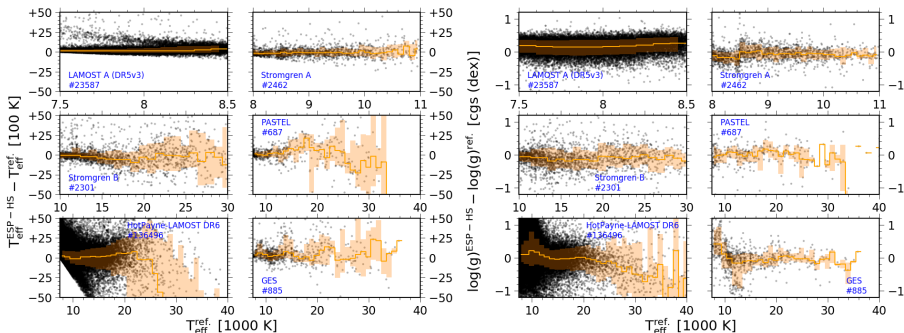
- Extinction: Fitzpatrick (1999),  $R_V = 3.1$
- Synthetic/Simulations spectra of reference of A and B stars (w. stromgren photometry) compared to Gaia XP data
- comparisons used to empirically improve the simulations, exclude domains
- no correlations taken into account

From GBP 3.00 to 14.00: A lib (5145 stars)



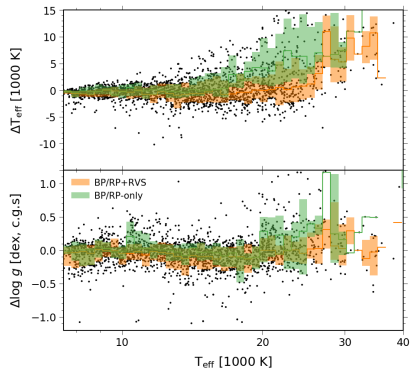
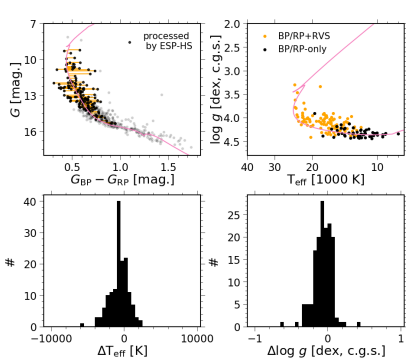


# AP Determination vs GroundBased Surveys



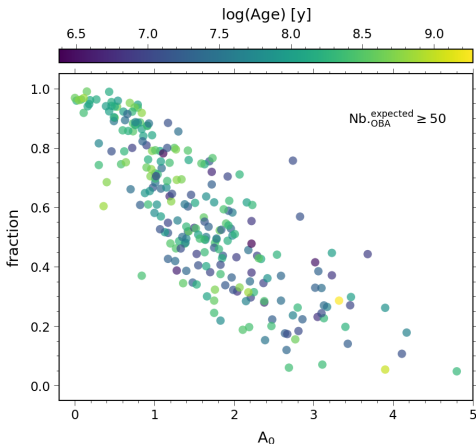
- in orange: median (line), interquartile dispersion (shades)
- $T_{\text{eff}}$ : trend to underestimate the temperature, especially above 25 000 K. Scatter increases with  $T_{\text{eff}}$  from 200-600 K (A-type), to 3000-10000 K (O-type).
- $\log g$ : dispersion 0.3-0.5, double for O-type stars.

# AP Determination vs Clusters



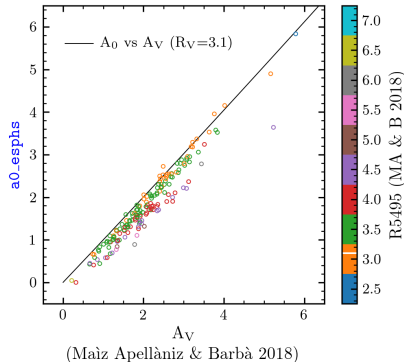
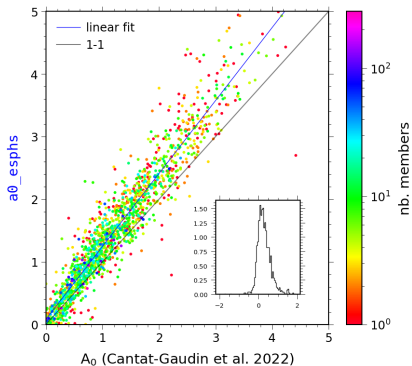
- Left: Case of NGC869, Right: 1524 members of 42 open clusters
- CD used to identify the closest isochrone point
- $T_{\text{eff}}$ : disp 800-6000 K;  $\log g$ : disp 0.15-0.30 dex

# Completeness of the OBA Sample from OCs



- Post-processing based on gof in XP and RVS (e.g 1/3rd of GOSC stars remaining).
- lack of stars trends with extinction

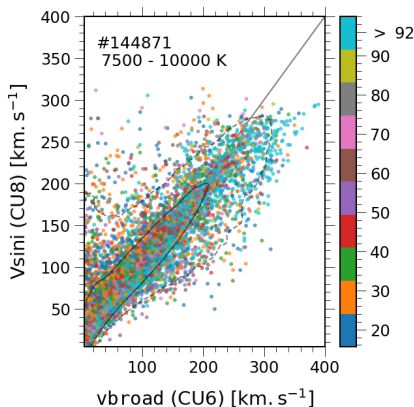
# Interstellar Reddening



- Fair agreement with other surveys and cluster data.
- left: comparison with OCs; right: comparison for O-type stars with different  $R_V$ . Different trends, expected trend with  $R_{5495}$ , as assumption is  $R_V=3.1$ .

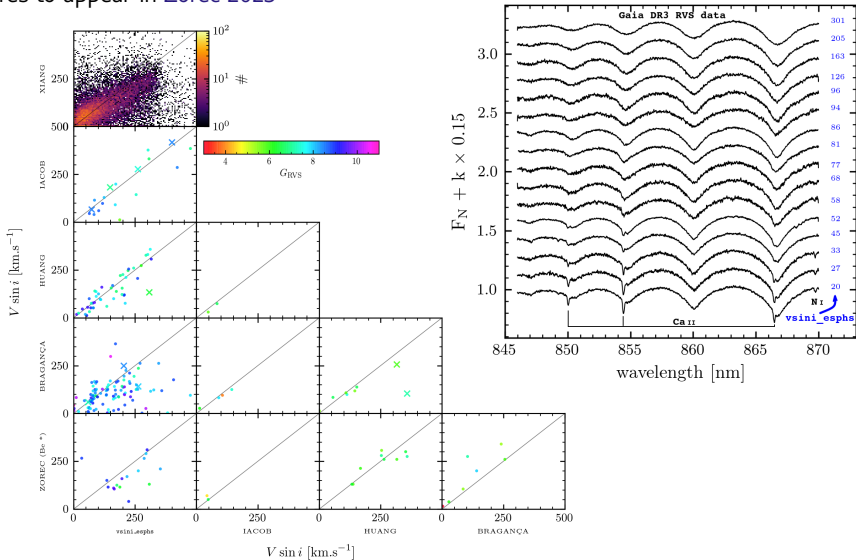
# $V_{\text{sin } i}$ Determination vs. epoch $v_{\text{broad}}$

- Performed on co-added spectra, assuming Gaussian LSF, in the AP determination.
- $v_{\text{sin } i\_esphs}$  larger than CU6/'epoch'  $v_{\text{broad}}$  at small values
- behaviour similar to  $v_{\text{broad}}$  (Frémat et al. 2022):  
The quality degrades rapidly with magnitude and  $T_{\text{eff}}$ , above  $G=10$  and  $T_{\text{eff}} > 10\,000\text{K}$ .
- see also Figure 20 in Foesneau et al. 2022



# $V \sin i$ Determination from co-added RVS

Figures to appear in Zorec 2023



# Overview & from DR3 to DR4

**gaia archive**

HOME SEARCH SINGLE OBJECT VISUALISATION HELP

Basic: **Advanced (ADQL)** Query Results

gaia

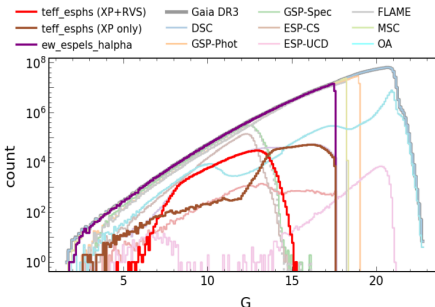
- Gaia Data Release 3
  - gaiaedr3.gaia\_source
  - gaiaedr3.gaia\_source\_tle
  - Astrophysical parameters
    - gaiaedr3.astrophysical\_parameters
      - flags\_gspspec
      - logchrng\_gspispec
      - ew\_esps\_halpha** *H $\alpha$*
      - ew\_esps\_halpha\_uncertainty
      - ew\_esps\_halpha\_flag
      - ew\_esps\_halpha\_model
      - classlabel\_esps** *ELS labelling*
      - classlabel\_esps\_flag
      - classprob\_esps\_wcstar
      - classprob\_esps\_wmstar
      - classprob\_esps\_bstar
      - classprob\_esps\_tauristar
      - classprob\_esps\_hertigstar
      - classprob\_esps\_dmstar
      - classprob\_esps\_pne
      - azero\_esps
      - azero\_esps\_uncertainty
      - ag\_esps** *APs and reddening*
      - ag\_esps\_uncertainty
      - etpminrp\_esps
      - etpminrp\_esps\_uncertainty
      - teff\_esps
      - teff\_esps\_uncertainty
      - logg\_esps
      - logg\_esps\_uncertainty
      - vsini\_esps** *RVS line broadening*
      - vsini\_esps\_uncertainty
      - flags\_esps
      - spectra1type\_esps** *2nd digit*
      - activityindex\_esps
      - activityindex\_esps\_uncertainty

## ■ ESP-ELS:

- DR4> probability of H $\alpha$  being in emission
- DR4> RVS included in the classification

## ■ ESP-HS:

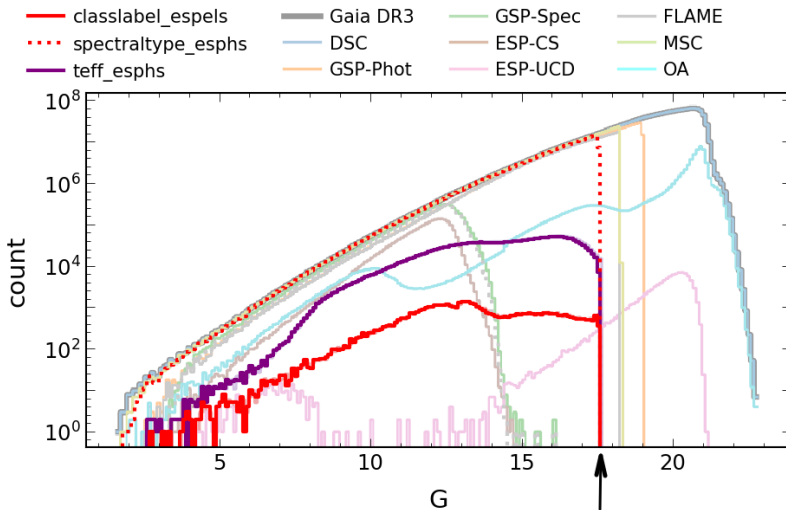
- DR4> Metallicity determination from RVS for A and late-B stars.
- DR4> Post-processing less restrictive.



# Thank you for your attention



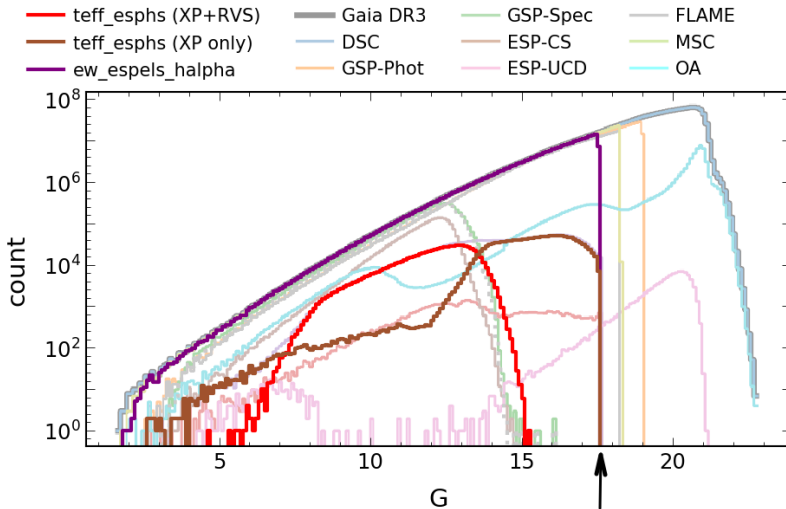
# Output: Magnitude Distribution



Adapted from Creevey et al. 2022, Figure 2

ESP-ELS/HS magnitude cut at G=17.65

# Output: Magnitude Distribution



Adapted from Creevey et al. 2022, Figure 2

ESP-ELS/HS magnitude cut at G=17.65